Journal of Organometallic Chemistry, 260 (1984) 347–362
Elsevier Sequoia S.A., Lausanne – Printed in The Netherlands

SYNTHESIS OF CHELATING TRIMETHYLSILOXY DIISONITRILE LIGANDS AND THEIR RHODIUM(I) COMPLEXES. CRYSTAL AND MOLECULAR STRUCTURE OF $[Rh(t\text{-}BuDiNC)_2]BPh_4 \cdot 1.5CH_3CN$ (DiNC = chelating bidentate isonitrile ligand)

DANIEL T. PLUMMER, BARBARA A. KARCHER, ROBERT A. JACOBSON, and ROBERT J. ANGELICI*

Department of Chemistry and Ames Laboratory-DOE, Iowa State University, Ames, Iowa 50011 (U.S.A.)

(Received April 5th, 1983)

Summary

An X-ray crystallographic study, the first of a complex containing a chelating bidentate isonitrile (DiNC) ligand, reveals that $[Rh(t\text{-}BuDiNC)_2]BPh_4 \cdot 1.5CH_3CN$ crystallizes as a "slipped-stacked" face-to-face dimer of two approximately planar $[Rh(t\text{-}BuDiNC)_2]^+$ cations with a Rh–Rh distance of 3.384 Å, and an angle of 22.7° between the stacking axis and the Rh–Rh vector. The syntheses of two new bidentate isonitrile ligands, SiNC-2 and SiNC-3 are also described. These ligands contain bulky trimethylsiloxy groups *ortho* to each isonitrile group and differ only in that the SiNC-3 ligand contains an additional CH_2 unit in its backbone. Each reacts with $[Rh(COD)Cl]_2$ to afford, after metathesis with KPF_6, a complex of the empirical formula $[Rh(SiNC\text{-}n)_2]PF_6$. Spectroscopic results suggest the SiNC-2 complex is dinuclear, with four SiNC-2 ligands bridging the two rhodium atoms. The SiNC-3 complex is mononuclear, but unlike most other mononuclear $[Rh(CNR)_4]^+$ complexes, shows no tendency to self-associate in solution. The different structures of these two complexes and the solution behavior of the SiNC-3 complex are attributed to the bulkiness of the trimethylsiloxy groups.

Introduction

Recently, we reported the synthesis of several potentially chelating ligands containing isonitrile [1–5], nitrile [1,3], and diazonium [6] donor groups. The

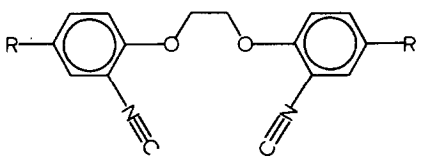

0022-328X/84/$03.00

chelating bidentate isonitrile ligands DiNC (for R = H) and t-BuDiNC (for R = t-Bu) have been shown to form stable complexes with many transition metals [1,3,5], including square-planar complexes of rhodium(I) [4]. Complexes of the general type $[Rh(CNR)_4]^+$ with monodentate isonitrile ligands have been the subject of a number of investigations because of their interesting chemical and spectroscopic properties. In solution, such compounds have been shown [7–11] to oligomerize through Rh–Rh interactions, giving rise to intensely colored solutions at higher concentrations. In the solid state as well, $Rh(CNR)_4^+$ complexes are often highly colored. Three compounds of the type $Rh(CNAr)_4^+$ have been investigated by X-ray diffraction [10,12] and shown to contain the dimeric structural units $Rh_2(CNAr)_8^{2+}$, which possess weak Rh–Rh interactions. In $[Rh_2(CNPh)_8](BPh_4)_2$, the phenyl rings of the isocyanide ligands are rotated out of the RhC_4 plane into a propeller-type configuration. In complexes of DiNC and t-BuDiNC, however, molecular models indicate that the phenyl rings should be confined to lie more nearly in the RhC_4 plane. Thus, stronger Rh–Rh interactions might be possible with chelating bidentate ligands than with analogous monodentate ones; evidence for stronger Rh–Rh interactions in $Rh_2(DiNC)_4^{2+}$ and $Rh_2(DiNC)_4I_2^{2+}$ was noted previously [4].

We wish to report here the results of an X-ray diffraction study of $[Rh_2(t\text{-}BuDiNC)_4](BPh_4)_2 \cdot 3CH_3CN$, the first structural investigation of a complex containing chelating bidentate isonitrile ligands [4]. Also described are the syntheses of two new bidentate isonitrile ligands and their rhodium(I) complexes. The SiNC-2

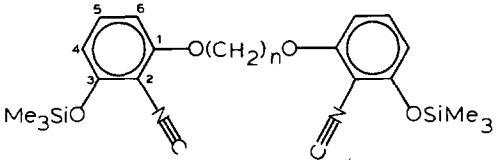

SiNC - 2 : n = 2

SiNC - 3 : n = 3

and SiNC-3 complexes were initially synthesized with the idea of coupling the ligands through their phenoxy oxygens to yield macrocyclic tetraisonitrilerhodium complexes. While these coupling reactions were unsuccessful, the complexes themselves are interesting because of the unanticipated effect of the bulky trimethylsiloxy groups on their structures.

Results and discussion

Description of the structure of $[Rh(t\text{-}BuDiNC)_2]BPh_4 \cdot 1.5CH_3CN$

In the solid state, $[Rh(t\text{-}BuDiNC)_2]BPh_4 \cdot 1.5CH_3CN$ is composed of discrete dimers of the $[Rh(t\text{-}BuDiNC)_2]^+$ unit. Computer-generated drawings of this unit and the unit cell are found in Fig. 1 and 2, respectively. Atomic coordinates, bond distances, and bond angles are listed in Tables 1–3. The dimeric cations are eclipsed and are inversion-related, with a Rh–Rh distance of 3.384 Å. The coordination geometry about the rhodium atom is very nearly square-planar, with C–Rh–C angles ranging from 87.5 to 90.6° (Table 3). There is a slight pyramidal distortion within the RhC_4 unit, as indicated by a calculation of its least-squares plane; the carbon atoms are displaced by an average of +0.03 Å from the mean plane, while the rhodium atoms are displaced by −0.11 Å toward one another. In $[Rh_2(CN\text{-}p\text{-}C_6H_4F)_8]^{2+}$, a similar distortion is found [12]. A contrasting situation exists for

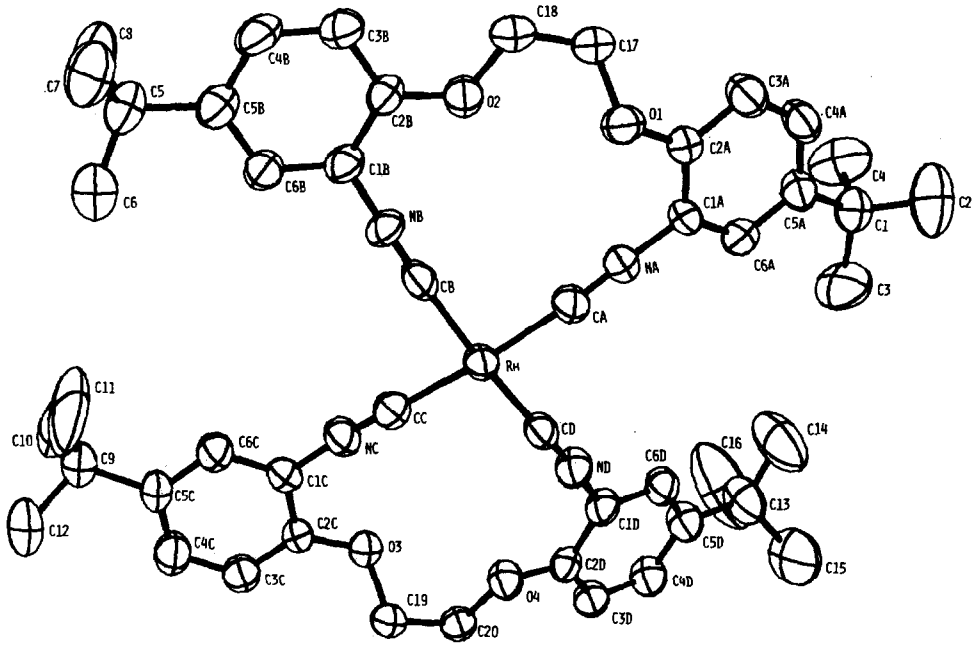

Fig. 1. ORTEP drawing of the $[Rh(t\text{-}BuDiNC)_2]^+$ unit.

$[Rh_2(CNC_6H_5)_8]^{2+}$, where distortions within the RhC_4 unit are roughly tetrahedral, rather than pyramidal, in nature [10].

The average rhodium–carbon bond distance of 1.965 Å in the present compound is comparable to those in other isonitrile complexes of rhodium: $[Rh_2(CNC_6H_5)_8](BPh_4)_2$ (1.94 Å) [10] $[Rh_2(CN(CH_2)_3NC)_4](BPh_4)_2 \cdot CH_3CN$ (1.96 Å) [13], $[Rh_2(CNC(CH_3)_2(CH_2)_2C(CH_3)_2NC)_4](PF_6)_2 \cdot 2\ CH_3CN$ (1.96 Å) [13], and $[Rh_2(CN\text{-}p\text{-}C_6H_4F)_8]Cl_2 \cdot 2H_2O$ (1.96 Å) [12]. The (C≡N) distance of 1.15 Å, as well as the Rh–C–N and C–N–C angles (175 and 173°, respectively), are also

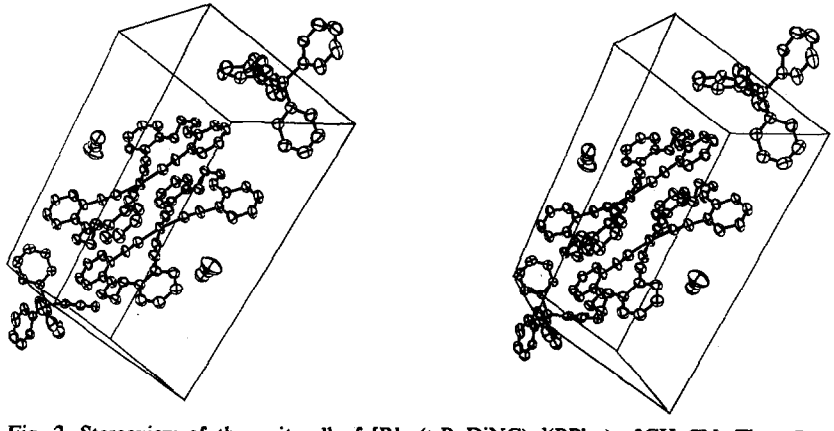

Fig. 2. Stereoview of the unit cell of $[Rh_2(t\text{-}BuDiNC)_4](BPh_4)_2 \cdot 3CH_3CN$. The t-Bu groups on the t-BuDiNC ligands are not shown for clarity.

TABLE 1

FINAL POSITIONAL PARAMETERS[a,b] FOR $[Rh_2(t\text{-}BuDiNC)_4](BPh_4)_2 \cdot 3CH_3CN$

Atom	x	y	z
(a) Final positional parameters for the cation			
Rh	0.54634(4)	0.54525(3)	0.3962(7)
C(A)	0.6716(4)	0.6080(4)	0.4406(7)
C(B)	0.5320(4)	0.6314(4)	0.4733(8)
C(C)	0.4189(5)	0.4880(4)	0.3300(8)
C(D)	0.5635(4)	0.4652(4)	0.3007(7)
N(A)	0.7438(4)	0.6472(3)	0.4576(6)
N(B)	0.5268(4)	0.6833(3)	0.5157(6)
N(C)	0.3453(4)	0.4542(3)	0.2865(6)
N(D)	0.5714(4)	0.4192(3)	0.2319(6)
C(1A)	0.8301(4)	0.6921(4)	0.4591(7)
C(2A)	0.8667(4)	0.7647(4)	0.5269(7)
C(3A)	0.9493(5)	0.8087(4)	0.5194(8)
C(4A)	0.9902(5)	0.7800(4)	0.4408(8)
C(5A)	0.9533(5)	0.7084(4)	0.3691(8)
C(6A)	0.8711(5)	0.6643(4)	0.3804(8)
C(1B)	0.5238(5)	0.7472(4)	0.5737(7)
C(2B)	0.5991(4)	0.8114(4)	0.6107(7)
C(3B)	0.5944(5)	0.8731(4)	0.6755(8)
C(4B)	0.5156(6)	0.8687(4)	0.6977(8)
C(5B)	0.4393(5)	0.8037(4)	0.6587(8)
C(6B)	0.4458(5)	0.7429(4)	0.5976(7)
C(1C)	0.2564(4)	0.4099(4)	0.2486(7)
C(2C)	0.2268(4)	0.3380(4)	0.1830(7)
C(3C)	0.1399(5)	0.2935(4)	0.1579(8)
C(4C)	0.0833(5)	0.3204(4)	0.1957(9)
C(5C)	0.1123(5)	0.3935(4)	0.2598(8)
C(6C)	0.2012(5)	0.4376(4)	0.2875(8)
C(1D)	0.5703(5)	0.3632(4)	0.1380(7)
C(2D)	0.4962(4)	0.2972(4)	0.1007(7)
C(3D)	0.4913(5)	0.2418(4)	0.0026(7)
C(4D)	0.5604(5)	0.2538(4)	−0.05611(8)
C(5D)	0.6351(5)	0.3196(4)	−0.0208(8)
C(6D)	0.6388(5)	0.3741(4)	0.0792(8)
C(1)	−0.9987(5)	0.6802(5)	0.2774(9)
C(2)	1.0903(8)	0.6996(9)	0.3529(13)
C(3)	0.9493(8)	0.5988(6)	0.2173(13)
C(4)	1.0020(9)	0.7154(6)	0.1649(11)
C(5)	0.3537(5)	0.8031(5)	0.6792(8)
C(6)	0.2817(7)	0.7264(6)	0.6470(13)
C(7)	0.3680(7)	0.8436(6)	0.8238(9)
C(8)	0.3252(7)	0.8425(6)	0.5907(10)
C(9)	0.0505(5)	0.4240(5)	0.2943(10)
C(10)	0.0159(12)	0.4424(11)	0.178(2)
C(11)	0.944(10)	0.4930(10)	0.402(2)
C(12)	−0.0265(9)	0.3691(8)	0.327(2)
C(13)	0.7075(6)	0.3293(5)	−0.0905(10)
C(14)	0.7844(9)	0.4013(8)	−0.034(2)
C(15)	0.6717(11)	0.318(2)	−0.232(2)
C(16)	0.7406(10)	0.2731(9)	−0.077(2)
C(17)	0.8219(5)	0.8563(4)	0.5856(8)
C(18)	0.7541(5)	0.8697(4)	0.64312(8)

TABLE 1 (continued)

Atom	x	y	z
C(19)	0.2838(5)	0.2519(4)	0.1664(8)
C(20)	0.3463(4)	0.2355(4)	0.1011(7)
O(1)	0.8193(3)	0.7885(2)	0.5974(5)
O(2)	0.6709(3)	0.8087(2)	0.5805(5)
O(3)	0.2864(3)	0.3175(3)	0.1424(5)
O(4)	0.4317(3)	0.2935(2)	0.1624(5)
(b) Final positional parameters for the anion and the solvent molecules			
B	0.7328(6)	−0.0343(5)	0.2895(8)
C(21)	0.7754(5)	0.0186(4)	0.1998(7)
C(22)	0.7581(8)	−0.0063(5)	0.0651(9)
C(23)	0.7897(10)	0.0379(6)	−0.0123(10)
C(24)	0.8399(8)	0.1106(6)	0.0428(11)
C(25)	0.8591(7)	0.1370(5)	0.1754(9)
C(26)	0.8279(5)	0.0920(4)	0.2530(8)
C(27)	0.7905(5)	0.0062(4)	0.4445(7)
C(28)	0.8712(5)	0.0087(4)	0.4876(8)
C(29)	0.9215(6)	0.0430(4)	0.6169(8)
C(30)	0.8919(6)	0.0766(4)	0.7075(8)
C(31)	0.8143(6)	0.0771(5)	0.6687(8)
C(32)	0.7627(5)	0.0429(4)	0.5387(8)
C(33)	0.7430(5)	−0.1095(4)	0.2475(7)
C(34)	0.6890(6)	−0.1741(4)	0.2708(8)
C(35)	0.7036(8)	−0.2346(5)	0.2536(9)
C(36)	0.7743(8)	−0.2337(5)	0.2093(9)
C(37)	0.8300(7)	−0.1719(6)	0.1827(9)
C(38)	0.8144(6)	−0.1117(5)	0.2031(8)
C(39)	0.6299(5)	−0.0520(4)	0.2760(7)
C(40)	0.5816(6)	−0.0391(4)	0.1739(8)
C(41)	0.4964(6)	−0.0505(5)	0.1689(9)
C(42)	0.4553(6)	−0.0744(6)	0.2630(11)
C(43)	0.5001(6)	−0.0887(6)	0.3596(11)
C(44)	0.5852(6)	−0.0776(5)	0.3669(9)
N(1)	0.2917(9)	0.4463(7)	0.910(2)
C(45)	0.3463(7)	0.4316(6)	0.9390(11)
C(46)	0.4104(8)	0.4123(7)	0.9693(13)
N(2)	0.071(2)	0.100(2)	0.073(3)

[a] Positional parameters are represented in fractional unit cell coordinates. [b] Standard deviations are given in parentheses.

unexceptional. Thus, there are no severe bond-angle deformations in the 13-membered t-BuDiNC chelate ring, suggesting that t-BuDiNC is well-suited for *cis*-coordination with C–M–C angles of ca. 90°. The phenyl rings of the t-BuDiNC ligands are slightly tipped with respect to the RhC_4 plane. Phenyl–RhC_4 interplanar angles have values of 24.8, 11.7, 6.4 and 31.1°, for phenyl rings A, B, C and D, respectively. A relatively short contact (3.54 Å) between C(34) of the BPh_4^- anion and C(3D) of phenyl ring D (3.01 Å between their hydrogens) may be partly responsible for the larger interplanar angle for ring D.

Rather than stacking directly over one another, the $[Rh(t\text{-}BuDiNC)_2]^+$ cations are shifted such that the rhodium atom of one cation lies considerably closer to the isonitrile carbon atom C(C) (3.18 Å) of the adjacent cation than to the inversion-re-

TABLE 2

BOND DISTANCES (Å) FOR $[Rh_2(t\text{-BuDiNC})_4]^{2+}$

Rh–C(A)	1.956(7)	C(2D)–C(3D)	1.38(1)
Rh–C(B)	1.976(7)	C(3D)–C(4D)	1.39(1)
Rh–C(C)	1.974(8)	C(4D)–C(5D)	1.39(1)
Rh–C(D)	1.955(7)	C(5D)–C(6D)	1.39(1)
C(A)–N(A)	1.150(9)	C(6D)–C(1D)	1.39(1)
C(B)–N(B)	1.146(9)	C(5A)–C(1)	1.53(1)
C(C)–N(C)	1.147(9)	C(1)–C(2)	1.52(2)
C(D)–N(D)	1.170(9)	C(1)–C(3)	1.54(1)
N(A)–C(1A)	1.406(8)	C(1)–C(4)	1.52(1)
N(B)–C(1B)	1.396(9)	C(5B)–C(5)	1.53(1)
N(C)–C(1C)	1.386(9)	C(5)–C(6)	1.52(1)
N(D)–C(1D)	1.390(9)	C(5)–C(7)	1.55(1)
C(1A)–C(2A)	1.39(1)	C(5)–C(8)	1.53(1)
C(2A)–C(3A)	1.38(1)	C(5C)–C(9)	1.51(1)
C(3A)–C(4A)	1.38(1)	C(9)–C(10)	1.50(2)
C(4A)–C(5A)	1.38(1)	C(9)–C(11)	1.49(2)
C(5A)–C(6A)	1.39(1)	C(9)–C(12)	1.52(2)
C(6A)–C(1A)	1.37(1)	C(5D)–C(13)	1.52(1)
C(1B)–C(2B)	1.38(1)	C(13)–C(14)	1.49(2)
C(2B)–C(3B)	1.39(1)	C(13)–C(15)	1.49(2)
C(3B)–C(4B)	1.39(1)	C(13)–C(16)	1.54(2)
C(4B)–C(5B)	1.40(1)	C(2A)–O(1)	1.369(8)
C(5B)–C(6B)	1.38(1)	O(1)–C(17)	1.446(8)
C(6B)–C(1B)	1.38(1)	C(17)–C(18)	1.504(11)
C(1C)–C(2C)	1.38(1)	C(18)–O(2)	1.437(9)
C(2C)–C(3C)	1.36(1)	O(2)–C(2B)	1.352(8)
C(3C)–C(4C)	1.40(1)	C(2C)–O(3)	1.368(8)
C(4C)–C(5C)	1.40(1)	O(3)–C(19)	1.443(8)
C(5C)–C(6C)	1.39(1)	C(19)–C(20)	1.489(10)
C(6C)–C(1C)	1.38(1)	C(20)–O(4)	1.435(8)
C(1D)–C(2D)	1.39(1)	O(4)–C(2D)	1.366(8)

lated Rh atom (3.384 Å). The distance between RhC_4 mean planes is 3.133 Å. Thus, the Rh–Rh vector forms an angle of 22.7° with the normal to the least squares RhC_4 plane. The Rh–Rh distance of 3.384 Å in $[Rh_2(t\text{-BuDiNC})_4]^{2+}$ is longer than that found in $[Rh_2(CNC_6H_5)_8]^{2+}$ (3.193 Å) [10] and the "bridge" complexes $[Rh_2(CN(CH_2)_3NC)_4]^{2+}$ (3.242 Å) [13] and $[Rh_2(CNC(CH_3)_2(CH_2)_2C(CH_3)_2NC)_4]^{2+}$ (3.262 Å) [13].

Certain aspects of the present structure are comparable to features found for $[Rh_2(CN\text{-}p\text{-}C_6H_4F)_8]Cl_2 \cdot 2H_2O$ [12] and $[Rh_2(CN\text{-}p\text{-}C_6H_4NO_2)_8]Cl_2$ [12]. Both of the latter complexes crystallize as eclipsed, dimeric units, $[Rh_2(CNR)_8]^{2+}$, with Rh–Rh distances of 3.207 and 3.25 Å, respectively. As with the t-BuDiNC complex, the cationic planes of the two compounds are "slipped" by angles of 13.844 and 31.5°, respectively. Interplanar phenyl–RhC_4 angles are quite small, having values from 2.2 to 11.1° for the *p*-fluorophenylisonitrile derivative. Thus, the $[Rh(CN\text{-}p\text{-}C_6H_4F)_4]^+$ unit is nearly planar.

The stacking relationship between pairs of $Rh(t\text{-BuDiNC})_2^+$ or $[Rh(CN\text{-}p\text{-}C_6H_4F)_4]^+$ units in the solid state is not unlike that found for many other planar systems, though often the latter have infinitely long stacks in the solid state. Infinite

TABLE 3

BOND ANGLES (°) FOR $[Rh_2(t\text{-BuDiNC})_4]^{2+}$

C(A)–Rh–C(B)	87.5(3)	N(C)–C(1C)–C(6C)	118.7(6)	C(6C)–C(5C)–C(9)	121.0(7)
C(A)–Rh–C(C)	171.6(3)	C(6C)–C(1C)–C(2C)	122.3(6)	C(5C)–C(9)–C(10)	108.6(10)
C(A)–Rh–C(D)	90.4(3)	C(1C)–C(2C)–C(3C)	118.0(6)	C(5C)–C(9)–C(11)	112.8(8)
C(B)–Rh–C(C)	90.6(3)	C(2C)–C(3C)–C(4C)	120.5(7)	C(5C)–C(9)–C(12)	111.2(8)
C(B)–Rh–C(D)	172.5(3)	C(3C)–C(4C)–C(5C)	122.0(7)	C(10)–C(9)–C(11)	105.4(12)
C(C)–Rh–C(D)	90.4(3)	C(4C)–C(5C)–C(6C)	116.7(7)	C(10)–C(9)–C(12)	107.6(11)
Rh–C(A)–N(A)	174.0(6)	C(5C)–C(6C)–C(1C)	120.5(7)	C(11)–C(9)–C(12)	110.9(12)
Rh–C(B)–N(B)	176.7(6)	N(D)–C(1D)–C(2D)	117.6(6)	C(4D)–C(5D)–C(13)	120.5(7)
Rh–C(C)–N(C)	177.3(7)	N(D)–C(1D)–C(6D)	120.8(6)	C(6D)–C(5D)–C(13)	122.8(7)
Rh–C(D)–N(D)	172.9(6)	C(6D)–C(1D)–C(2D)	121.5(7)	C(5D)–C(13)–C(14)	113.0(9)
C(A)–N(A)–C(1A)	171.9(7)	C(1D)–C(2D)–C(3D)	118.8(6)	C(5D)–C(13)–C(15)	108.7(9)
C(B)–N(B)–C(1B)	176.8(7)	C(2D)–C(3D)–C(4D)	119.0(7)	C(5D)–C(13)–C(16)	109.5(9)
C(C)–N(C)–C(1C)	172.3(8)	C(3D)–C(4D)–C(5D)	123.2(7)	C(14)–C(13)–C(15)	110.3(13)
C(D)–N(D)–C(1D)	172.0(7)	C(4D)–C(5D)–C(6D)	116.7(7)	C(14)–C(13)–C(16)	106.4(10)
N(A)–C(1A)–C(2A)	118.8(6)	C(5D)–C(6D)–C(1D)	120.8(7)	C(15)–C(13)–C(16)	108.9(14)
N(A)–C(1A)–C(6A)	118.4(6)	C(6A)–C(5A)–C(1)	121.8(7)	C(1A)–C(2A)–O(1)	118.4(6)
C(6A)–C(1A)–C(2A)	122.2(6)	C(4A)–C(5A)–C(1)	121.5(7)	C(3A)–C(2A)–O(1)	123.8(6)
C(1A)–C(2A)–C(3A)	117.8(6)	C(5A)–C(1)–C(2)	109.3(8)	C(2A)–O(1)–C(17)	115.0(5)
C(2A)–C(3A)–C(4A)	119.3(7)	C(5A)–C(1)–C(3)	112.1(8)	O(1)–C(17)–C(18)	110.4(6)
C(3A)–C(4A)–C(5A)	123.5(7)	C(5A)–C(1)–C(4)	108.0(8)	C(17)–C(18)–O(2)	108.3(6)
C(4A)–C(5A)–C(6A)	116.6(7)	C(2)–C(1)–C(3)	109.2(10)	C(18)–O(2)–C(2B)	118.4(5)
C(5A)–C(6A)–C(1A)	120.5(7)	C(2)–C(1)–C(4)	110.6(9)	C(1B)–C(2B)–O(2)	117.0(6)
N(B)–C(1B)–C(2B)	119.1(6)	C(3)–C(1)–C(4)	107.6(9)	C(3B)–C(2B)–O(2)	125.8(6)
N(B)–C(1B)–C(6B)	118.3(6)	C(4B)–C(5B)–C(5)	120.0(7)	C(1C)–C(2C)–O(3)	117.2(6)
C(6B)–C(1B)–C(2B)	122.5(6)	C(6B)–C(5B)–C(5)	123.4(7)	C(3C)–C(2C)–O(3)	124.7(6)
C(1B)–C(2B)–C(3B)	117.2(6)	C(5B)–C(5)–C(6)	111.4(7)	C(2C)–O(3)–C(19)	116.3(5)
C(2B)–C(3B)–C(4B)	120.1(7)	C(5B)–C(5)–C(7)	109.1(7)	O(3)–C(19)–C(20)	107.2(6)
C(3B)–C(4B)–C(5B)	122.6(7)	C(5B)–C(5)–C(8)	109.6(7)	C(19)–C(20)–C(4)	107.7(6)
C(4B)–C(5B)–C(6B)	116.5(7)	C(6)–C(5)–C(7)	109.6(8)	C(20)–O(4)–C(2D)	117.3(5)
C(5B)–C(6B)–C(1B)	121.2(7)	C(6)–C(5)–C(8)	108.7(8)	C(1D)–C(2D)–O(4)	116.3(6)
N(C)–C(1C)–C(2C)	118.7(6)	C(7)–C(5)–C(8)	108.4(8)	C(3D)–C(2D)–O(4)	124.9(6)
		C(4C)–C(5C)–C(9)	122.3(7)		

"slipped-stacked" packing arrangements are found in simple aromatic hydrocarbons such as coronene [14], a number of organic donor–acceptor π-molecular complexes [15], as well as transition-metal α,β-dionedioximates [16] and transition metal phthalocyanines [16]. For the latter two cases, where metal–metal interactions are possible, it has been suggested that Van der Waal's interactions and packing forces are dominant over metal–metal interactions in determining the solid state structures [16]. It is quite possible that similar forces are operative in the $[Rh(t\text{-BuDiNC})_2]^+$ and $[Rh(CN\text{-}p\text{-}C_6H_4F)_4]^+$ systems.

The structures of $[Rh_2(t\text{-BuDiNC})_4](BPh_4)_2 \cdot 3CH_3CN$, $[Rh_2(CN\text{-}p\text{-}C_6H_4F)_8]Cl_2 \cdot 2\ H_2O$ and $[Rh_2(CN\text{-}p\text{-}C_6H_4\text{-}NO_2)_8]Cl_2$ can be contrasted with the structure of $[Rh_2(CNC_6H_5)_8](BPh_4)_2$ [10]. The dimeric units, $[Rh_2(CNPh)_8]^{2+}$, found in this compound are composed of staggered, rather than eclipsed, $[Rh(CNPh)_4]^+$ cations with a relatively short Rh–Rh distance of 3.193 Å (vide supra). In this case, there is no "slippage" of the cationic units; the Rh–Rh vector is coincident with the stacking axis. The staggered phenyl substituents in $[Rh_2(CNPh)_8]^{2+}$ are tipped with respect to the RhC_4 plane, with phenyl–RhC_4 interplanar angles that range from 22.9 to

71.8°. For this compound, it would appear that Van der Waal's forces between the cations $[Rh(CNPh)_4]^+$ are unimportant relative to the rhodium–rhodium bond in stabilizing the dimeric unit in the solid state.

Ligand synthesis

The new bidentate isonitrile ligands SiNC-2 and SiNC-3 were prepared as shown in Scheme 1 in overall yields of 14 and 34%, respectively. Coupling of two

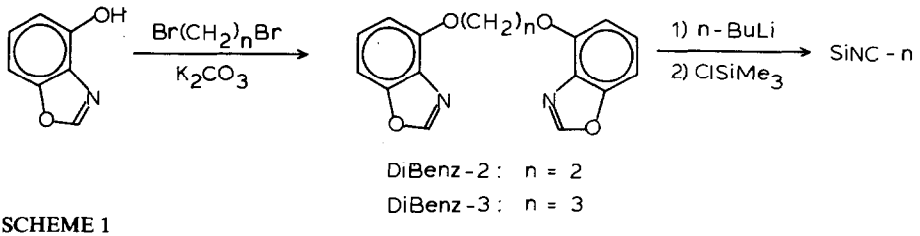

SCHEME 1

4-hydroxybenzoxazole units with the appropriate α,ω-dibromoalkane yielded the dibenzoxazole compounds Dibenz-2 and -3. In the following reaction, the benzoxazole functionality reacted with n-BuLi at low temperature in THF solution, yielding the 2-lithiobenzoxazole. At 0°C, the oxazole ring of this anion apparently opens to the 2-isocyanophenoxide, which is silylated exclusively at oxygen by $ClSiMe_3$, to yield the *o*-trimethylsiloxyisocyanophenyl units found in the final products, SiNC-2 and -3. A similar reaction of 4,5-diphenyloxazole with n-BuLi and $ClSiMe_3$ was shown earlier by Schöllkopf and coworkers to form *cis*- and *trans*-1,2-diphenyl-2-trimethylsiloxyvinyl isonitriles [17].

Analysis of the products SiNC-2 and -3 by ^1H or ^{13}C NMR showed that each usually contained about 10% of the unreacted benzoxazole due either to incomplete reaction or hydrolysis of the silyl ether by adventitious water (vide infra). However, products of this purity were suitable for further reactions without additional purification. The diisonitrile ligands thus obtained are colorless to pale yellow, odorless solids. As solids, they react slowly over a period of weeks with atmospheric moisture via hydrolysis of the silyl ether to regenerate the benzoxazole and hexamethyldisiloxane. In $CDCl_3$ solution, a similar decomposition reaction with CH_3OH took place over a period of about 8 h, giving the dibenzoxazole precursor and $MeOSiMe_3$. In the solid state, SiNC-2 and -3 have isonitrile stretching frequencies of 2130 and 2126 cm^{-1}, respectively, which are normal values for aromatic isonitriles [18].

The ligands are only slightly soluble in saturated hydrocarbons; the solubility of SiNC-3 is noticeably greater than that of SiNC-2. Both are moderately soluble in diethyl ether and benzene, and are quite soluble in $CHCl_3$ and CH_2Cl_2.

Rhodium complexes

SiNC-2 and -3 reacted at room temperature in benzene solution with $[Rh(COD)Cl]_2$ to precipitate the hygroscopic blue (SiNC-2) and yellow-green (SiNC-3) chloride salts "$[Rh(L–L)_2]Cl$". Metathesis with $NaBPh_4$ or KPF_6 gave products having the empirical formulae $[Rh(SiNC\text{-}2)_2]X$ ($X = BPh_4$, PF_6) and $[Rh(SiNC\text{-}3)_2]PF_6$ as analytically pure solids. The solid complexes containing the ethylene-bridged ligand are deep blue-green, while the SiNC-3 complex is green in color.

TABLE 4

ELECTRONIC SPECTRA OF RHODIUM(I) COMPLEXES, nm ($\epsilon \times 10^{-3}$ M cm)

Compound	Monomer absorptions				Dimer absorptions	
	$^1A_{1g} \rightarrow {}^1E_u$	$^1A_{1g} \rightarrow {}^3E_u$	$^1A_{1g} \rightarrow {}^1A_{2u}$	$^1A_{1g} \rightarrow {}^3A_{2u}$	$^1A_{1g} \rightarrow {}^1E_u$	$^1A_{1g} \rightarrow {}^1A_{2u}$
$[Rh(SiNC\text{-}3)_2]^+$ [a]	352 (35)	[b]	406 (2.8)	463 (0.6)		
$[Rh_2(SiNC\text{-}2)_4]^{2+}$ [a]					362 (36.8)	607 (4.4)
$[Rh(DiNC)_2]^+$ [c]	357 (70.1)	415 sh	427 (6.1)	472 (1.1)	[d]	602 (18.6)
$[Rh(t\text{-}BuDiNC)_2]^+$ [c]	361 (66.5)	413 sh	421 (5.2)	472 (1.2)	[d]	612 (14.5)
$[Rh(CNPh)_4]^+$ [e]	335 (48)	[b]	411 (5.7)	463 (0.66)	[d]	568 (8.5–12.5)
$[Rh_2(CN(CH_2)_3NC)_4]^{2+}$ [f]					318 (31.5) [g]	553 (14.5)

[a] CH_3CN solution. [b] Not observed. [c] DMF solution, ref. 4. [d] Probably coincident with monomer transition. [e] CH_3CN solution, ref. 10. [f] CH_3CN solution ref. 13. [g] $^1A_{1g} \rightarrow {}^3E_u$ band at 344 nm (5.5).

Infrared spectra of the rhodium(I) complexes $[Rh_2(SiNC\text{-}2)_4]^{2+}$ and $[Rh(SiNC\text{-}3)_2]^+$ exhibit a strong ν(C≡N) band at ca. 2160 cm^{-1}, about 30 cm^{-1} higher in energy than that observed for the free ligands. Similar shifts in ν(C≡N) are observed in analogous systems containing aliphatic [7,9,10,11,19] or aromatic isonitriles [4,10,20,21]. In addition, a weak shoulder is also seen at 2200 cm^{-1} in each case. This band is probably due to a weakly-allowed mode of a_{1g} or b_{1g} symmetry [20,21]. Other characteristic infrared bands include the strong ν(SiO) absorbance of the silyl ether at ca. 840 cm^{-1}. In spectra of the PF_6^- salts, this band is coincident with ν(PF) of the counter ion.

The structures of these complexes can be evaluated in terms of their electronic

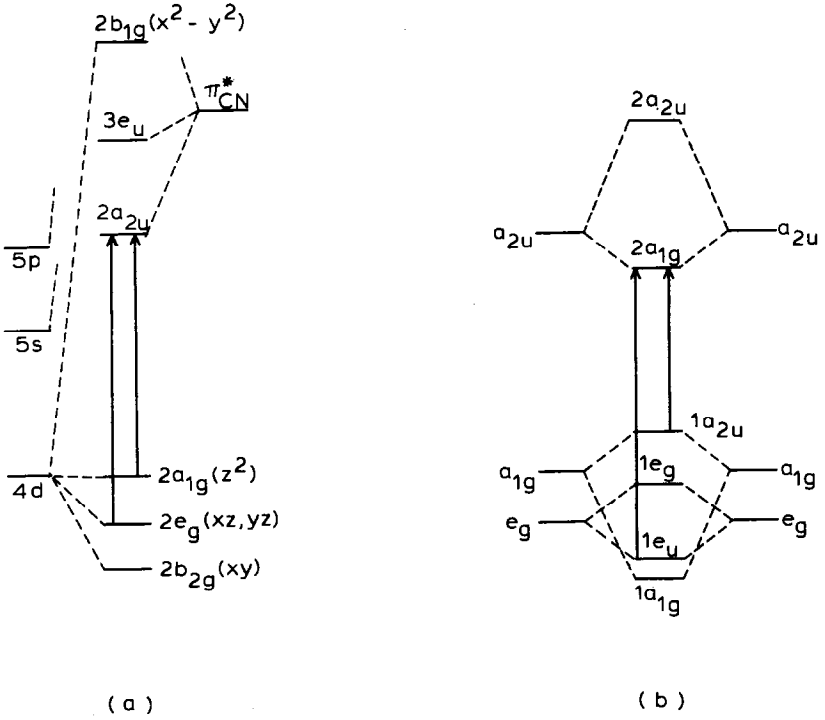

Fig. 3. Qualitative molecular orbital diagrams for (a) $[Rh(CNR)_4]^+$ and (b) $[Rh_2(CNR)_8]^{2+}$.

spectra. The $[Rh(SiNC\text{-}3)_2]^+$ cation has a spectrum comparable to those of other monomeric $[Rh(CNR)_4]^+$ complexes (Table 4). In CH_3CN solution, three bands are observed at 352, 406, and 463 nm, assigned to the transitions $^1A_{1g} \rightarrow {}^1E_u$ ($2e_g \rightarrow 2a_{2u}$), $^1A_{1g} \rightarrow {}^1A_{2u}$ ($2a_{1g} \rightarrow 2a_{2u}$), and $^1A_{1g} \rightarrow {}^3A_{2u}$ ($2a_{1g} \rightarrow 2a_{2u}$), respectively. These transitions can be seen in Fig. 3a, which shows a MO diagram adapted from that of Geoffroy et al. [22]. At concentrations as high as 3×10^{-3} *M*, $[Rh(SiNC\text{-}3)_2]^+$ shows no tendency to dimerize, as evidenced by the lack of a low-energy band at ca. 600

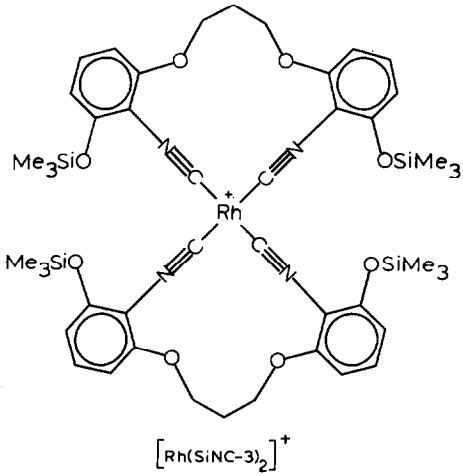

nm in its electronic spectrum (vide infra). In contrast, solutions of the SiNC-2 complex form blue-green solutions with only two absorption maxima, at 362 and 607 nm (Table 4). The two bands appear to arise solely from transitions within a weakly Rh–Rh-bound dimer, with bands being assigned to the transitions $^1A_{1g} \rightarrow {}^1E_u$ ($1e_u \rightarrow 2a_{1g}$) and $^1A_{1g} \rightarrow {}^1A_{2u}$ ($1a_{2u} \rightarrow 2a_{1g}$), respectively. These transitions can be seen in the MO diagram of Fig. 3b, which shows the mixing of the d_{z^2} ($2a_{1g}$) and π^*_{CN} ($2a_{2u}$) orbitals, as described by Mann et al. [8,10], as well as mixing of the d_{xz}, d_{yz} ($2e_g$) orbitals, which probably also occurs. No bands assignable to transitions within a $[Rh(SiNC\text{-}2)_2]^+$ monomer (i.e. at ca. 410 and 460 nm) are observed, nor is the observed spectrum dependent upon concentration over the range 2.8×10^{-3} to 5.6×10^{-6} *M*. Thus, it seems most likely that $[Rh_2(SiNC\text{-}2)_4]^{2+}$ exists as a dimer containing four bridging SiNC-2 ligands, as shown below. The $[Rh_2(SiNC\text{-}2)_4]^{2+}$ dication appears to be the first example of a dinuclear rhodium(I) complex containing bridging aromatic diisonitrile ligands, though there are a number of dinuclear rhodium complexes containing bridging aliphatic diisonitriles [7,9,11,13,23].

An interesting question concerns the very different structures and solution behaviors of the rhodium(I) complexes of the bidentate isonitrile ligands DiNC, t-BuDiNC, SiNC-2, and SiNC-3. As reported previously [4], the $[Rh(DiNC)_2]^+$ and $[Rh(t\text{-}BuDiNC)_2]^+$ monomers form dimers (and in the case of $[Rh(DiNC)_2]^+$, higher oligomers) at concentrations greater than 1×10^{-4} *M*. The $[Rh(CNPh)_4]^+$ monomer likewise forms oligomers in solution at concentrations greater than 5×10^{-4} *M*. $[Rh(SiNC\text{-}3)_2]^+$ has shown no evidence of solution oligomerization at concentrations of up to 3×10^{-3} *M*. The formation of oligomers in the case of $[Rh(SiNC\text{-}3)_2]^+$ is thought to be precluded by the steric bulk of the trimethylsiloxy groups. Molecular models suggest that the 14-membered Rh/SiNC-3 chelate rings are capable of

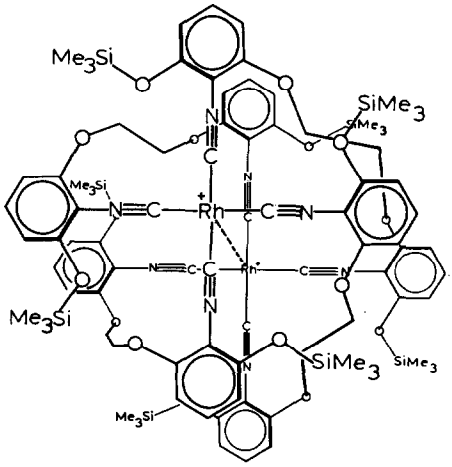

undergoing significant distortions in order to relieve unfavorable steric interactions between facing pairs of trimethylsiloxy groups in the two SiNC-3 ligands. In doing so, these groups (and perhaps the propylene units as well) must project far enough above and below the RhC_4 plane to inhibit the oligomerization process. Steric effects have been shown previously to affect oligomerization behavior, as with tetrakis(2,4,6-tri-t-butylphenylisonitrile)rhodium(I), which shows no tendency to dimerize [24].

The formation of a SiNC-2-bridged complex $Rh_2(SiNC\text{-}2)_4^{2+}$ from the reaction of SiNC-2 with $[Rh(COD)Cl]_2$ is probably a result of steric effects also. In molecular models of $[Rh(SiNC\text{-}2)_2]^+$, the phenyl units of the rigid chelate ring cannot be twisted sufficiently to avoid unfavorable interactions between opposing trimethylsiloxy groups in the two SiNC-2 ligands. These interactions are apparently so destabilizing that the SiNC-2-bridged structure, which involves no close contacts among the trimethylsiloxy groups, is favored.

Proton NMR spectra of the complexes are similar to those of the free ligands themselves, though the CH_2CH_2 resonance of $[Rh_2(SiNC\text{-}2)_4]^{2+}$ is slightly broadened relative to free SiNC-2. The SiNC-2 complex probably has an instantaneous solution structure of D_4 symmetry, since a Rh–Rh interaction would probably bring the Rh atoms to a bonding distance of ca. 3.3 Å. In this chiral structure, the CH_2CH_2 protons might be characterized as an AA'BB' spin system, as the two protons on a given methylene group are not interconverted by any symmetry operation. The single CH_2CH_2 resonance suggests that either the Δ/Λ interconversion is fast (greater than several hundred Hz) or that the asymmetry between methylene protons is only very slight. In NMR spectra of $[Rh(SiNC\text{-}3)_2]^+$, the OCH_2 and CH_2 signals are seen as a triplet and multiplet, respectively, with chemical shift values close to those of the free ligand.

Experimental

Crystal data

$RhO_4N_4C_{72}BH_{76} \cdot 1.5NC_2H_3$, M.W. = 1235.2, triclinic, $P\bar{1}$, a 17.355(8), b

21.135(10), c 10.757(5) Å, α 101.29(5), β 98.36(5), γ 113.92(4)°, V 3424.15 Å^3, ρ_c 1.22 g cm^{-3}, $Z = 2$, μ 3.33 cm^{-1} (Mo-K_α, λ 0.71034 Å).

Red-violet crystals of $[Rh_2(t\text{-BuDiNC})_4](BPh_4)_2$ were obtained by Dr. M.L. Winzenburg by slow evaporation of a CH_3CN solution of the complex in vacuo. The preparation of $[Rh_2(t\text{-BuDiNC})_4](BPh_4)_2$ is described elsewhere [4]. A prismatic crystal with approximate dimensions $0.4 \times 0.2 \times 0.15$ mm was mounted in a Lindemann glass capillary and glued in place with Duco cement.

Initial ω-oscillation photographs verified the crystal was single. From these pictures, 15 reflections were chosen as input for an auto-indexing procedure [25]. The resulting cell scalars indicated triclinic symmetry. The absence of mirror symmetry and the predicted reciprocal lattice spacings were confirmed by ω-oscillation photographs about each axis.

Fifteen high-angle reflections were used to obtain accurate cell parameters and their standard deviations. A least-squares fit was done on their $\pm 2\theta$ values, which were measured on a previously-aligned four-circle diffractometer.

Collection and reduction of intensity data

Room-temperature data were collected using the Ames Laboratory fully-automated four-circle diffractometer [26]. Backgrounds were measured by offsetting 0.75° in ω. Scans were done by beginning at the calculated peak center and stepping until the minimum of the two background values, measured as noted above, was reached. Counting times were 1.0 second per 0.01° step in ω. All data within a 2θ sphere of 45° were measured with reflected-beam graphite monochromated Mo-K_α radiation (λ 0.71034 Å). A total of 10257 reflections were collected in the hkl, $\bar{h}\bar{k}l$, $\bar{h}k\bar{l}$, and $h\bar{k}\bar{l}$ octants using an ω-stepscan technique.

Initially, four reflections were remeasured after every 75 reflections as a check on crystal and electronic stability. These standards decayed considerably during the first portion of data collection in which 675 reflections were measured. After this period, the crystal stabilized; this was indicated by three standards whose intensities no longer varied appreciably during the completion of data collection. The fourth standard was eliminated after 675 reflections, because of its low intensity. The decay, based on the integrated intensities of three standards, was fit to a quadratic polynomial: $y(x) = 0.7027 + 0.0008421\ x + 0.0000001495\ x^2$, where x is the reflection number and $y(x)$ is a multiplier for the intensity of each reflection. The first portion of the data was rescaled in this manner. During the total period of data collection, a decay in these standards of 35% was noted.

A Howells, Phillips, and Rogers test [27] indicated the structure has a center of symmetry. Thus, the space group was assumed to be $P\bar{1}$. The data were corrected for Lorentz and polarization effects. Each intensity's variance was calculated by

$$\sigma_I^2 = C_T + k_B C_B + (0.03\ C_T)^2 + (0.03\ C_B)^2,$$

where C_T, C_B and k_B are the total count, background count, and a counting time factor, respectively, and the 0.03 factor is an estimate of non-statistical errors. The finite difference method [28] was used to compute the estimated deviations in the structure factors. A reflection was considered observed if $I > 3\sigma(I)$; after equivalent data were averaged, there were 5912 reflections which met this requirement.

The calculated minimum and maximum transmittances are 0.88 and 0.95, respec-

tively. In light of the relatively high transmission and the small (3.8%) deviation from the average, no absorption correction was made.

Solution and refinement

The position of the rhodium atom was determined by the analysis of a sharpened Patterson function. A single superposition was then done by using the rhodium–rhodium vector. From the resultant map most of the non-hydrogen atoms were found. Their positions were put into a block-diagonal structure factor least-squares program [29]; a sharpened electron density map [30] based on this refinement readily revealed the positions of the remaining non-hydrogens. Electron density difference maps were then used to locate hydrogen atoms. Several groups of methyl hydrogens were not found on these maps probably due to low barriers to rotation; hence, they were not used in the refinement. The thermal parameters for the hydrogens were set equal to 4.0 $Å^2$; neither the thermal nor the positional parameters were varied in refinement.

The block-matrix least-squares minimized the function $\Sigma\omega(|F_o| - |F_c|)^2$, where $\omega = 1/\sigma(F^2)$. The function $\overline{\omega(|F_o| - |F_c|)^2}$ should be a constant with respect to $|F_o|$ and $\sin\theta/\lambda$ [31]. An analysis of the weights (ω) indicated some overweighting at very low and very high $\sin\theta/\lambda$ values; these values were subsequently adjusted. The conventional residual index, $R = \Sigma||F_o| - |F_c||/\Sigma|F_o|$, was equal to 8.1%.

The difference map still had two large peaks near the origin. Their maxima were about 1.14 Å apart. The peak nearest the origin, where there is an inversion center, was 1.45 Å from its symmetry-related partner. These peaks were resolved as a disordered acetonitrile molecule. The nitrogen sits at x, y, z half the time and $\bar{x}, \bar{y}, \bar{z}$ the remainder of the time. The positions of the methyl carbon and the nitrile carbon are inversion-related; the position of the nitrogen at any given time distinguishes them.

After this group was refined, a final residual index of 7.0% resulted. The weighted residual, $R_\omega = (\Sigma\omega(F_o - F_c)^2/\Sigma\omega F_o^2)^{1/2}$, was equal to 7.9%. The scattering factors used in the refinement were those of Hanson et al. [32], the rhodium factors were modified for anomalous dispersion effects [33]. The hydrogen scattering factors of Stewart et al. [34] were used. A list of calculated and observed structure factor amplitudes is available from the authors.

Syntheses-general information

Tetrahydrofuran (THF) and diethyl ether were distilled from Na/benzophenone ketyl under N_2 immediately before use. Dichloromethane and $ClSiMe_3$ were distilled from CaH_2 prior to use. Acetonitrile was stirred over CaH_2 overnight and distilled successively from P_4O_{10} and CaH_2. *N,N*-Dimethylformamide (DMF) was purged for 30 minutes with dry N_2. Benzene was stirred over H_2SO_4 and fractionally distilled. Hexane was distilled from P_4O_{10}. Dichlorodi-1,5-cyclooctadienedirhodium ($[Rh(COD)Cl]_2$) [35] and 4-hydroxybenzoxazole [36] were prepared by the cited methods. All other chemicals were used as received.

Preparations and reactions of the metal complexes were carried out under an atmosphere of N_2 (dried over 4A molecular sieves) in Schlenkware or similar apparatus using standard inert atmosphere techniques [37]. Infrared spectra were recorded on a Perkin–Elmer 281 infrared spectrophotometer. All NMR spectra were recorded on a JEOL FX-90Q NMR spectrometer. Chemical shifts are reported in ppm downfield from internal TMS. Visible-UV spectra were obtained with a

Perkin–Elmer 320 spectrophotometer. Melting points were measured on a Thomas hot stage and are uncorrected.

Ligand preparations

1,2-Bis(4,4'-benzoxazoloxy)ethane, Dibenz-2. In 20 ml of DMF under N_2, 4-hydroxybenzoxazole (6.75 g, 50.0 mmol), K_2CO_3 (7.00 g, 50.0 mmol), and 1,2-dibromoethane (2.15 ml, 4.70 g, 25.0 mmol) were heated at 65°C. After 25 h, an additional 1.0 ml of dibromoethane was added, and the mixture was heated for 22 h more. The reaction was cooled to 25°C and poured into 120 ml of rapidly-stirred ice water. The resulting white powder was filtered, washed repeatedly with H_2O, and then dried in vacuo. Excess starting material (ca. 2.5 g) was removed via sublimation (0.05 torr, 125°C). The residue was decolorized with activated charcoal and recrystallized from hot acetone to give the product as colorless needles (3.07 g, 41%), m.p. 163–165°C. MS: M^+ (*m/e* 296, 0.6%); $(C_9H_8NO_2)^+$, (*m/e* 162, 100%). ^1H NMR (acetone-d_6): δ 8.35 (s, OCH=N); 7.37–6.97 (m, ArH); 4.82 (s, CH_2). ^{13}C NMR ($CDCl_3$): 151.8 (Cl, C3); 151.0 (OCHN); 127.5 (C2); 126.3 (C5); 108.7 (C6); 104.0 (C4); 68.1 (OCH_2). Anal. Found: C, 64.75; H, 4.08; N, 9.35. $C_{16}H_{12}N_2O_4$ calcd.: C, 64.86; H, 4.08; N, 9.45%.

1,3-Bis(4,4'-benzoxazoloxy)propane, Dibenz-3. A procedure analogous to that above, starting with 3.00 g (22.2 mmol) of 4-hydroxybenzoxazole, 3.00 g (21.4 mmol) of K_2CO_3 and 1.1 ml (2.2 g, 11 mmol) of 1,3-dibromopropane in 12 ml of DMF gave the product (3.34 g, 63%) as colorless needles, m.p. 128–129°C. MS: M^+ (*m/e* 310, 2.1%); $[C_{10}H_{10}NO_2]^+$ (*m/e* 176, 100%). ^1H NMR ($CDCl_3$): δ 8.00 (s, CH); 7.40–6.75 (m, ArH); 4.50 (t, OCH_2); 2.48 (pentet, CH_2). ^{13}C NMR ($CDCl_3$): 151.4 (C1, C3); 150.9 (OCHN); 129.6 (C2); 126.1 (C5); 107.6 (C6); 103.4 (C4); 65.7 (OCH_2); 29.3 (CH_2). Anal. Found: C, 65.66; H, 4.63; N, 8.99. $C_{17}H_{14}N_2O_4$ calcd.: C, 65.80; H, 4.55; N, 9.03%.

1,2-Bis[2-isocyano-3-(trimethylsiloxy)phenoxy]ethane, SiNC-2. A sample of Dibenz-2 (1.91 g, 6.44 mmol) was suspended in 100 ml of THF under N_2, and the solution was cooled to −78°C. Over a period of five min, 5.90 ml (14.2 mmol) of a 2.4 *M* solution of n-BuLi in hexane was added, giving a yellow suspension. The mixture was stirred at −78°C for 20 min, then slowly warmed to 0°C, during which time a deep yellow-brown precipitate of the dianion formed. After stirring an additional 15 min at 0°C, 1.80 ml (1.54 g, 14.2 mmol) of $ClSiMe_3$ was added over a five minute period. The resulting yellow solution was stirred for 15 min at 0°C; then the solvent was removed at reduced pressure. The solid residue was treated with 10 ml of hexane at −10°C, and the resulting suspension was transferred via a cannula tube to a frit and filtered. This procedure was repeated once. The resulting solid was washed twice with 4 ml of hexane and the washes were discarded. The remaining pale yellow solid was extracted with three 5 ml portions of Et_2O, leaving LiCl on the frit. The ether solution was taken to near dryness, treated with 10 ml of hexane and cooled to −20°C to give the product as an off-white microcrystalline solid (0.991 g, 35%) after decantation of the mother liquor and drying in vacuo. In air, the solid melts at 100–107°C, then resolidifies and melts again at 162°C (the melting point of Dibenz-2). MS: M^+ (*m/e* 440, 5.8%); $(C_9H_8NO_2)^+$ (*m/e* 162, 62%); $[Si(CH_3)_3]^+$ (*m/e* 73, 100%). IR (Nujol mull): 2130 cm^{-1} s, ν(C≡N); 843 vs, ν(SiO). ^1H NMR ($CDCl_3$): δ 7.29–6.48 (m, ArH); 4.47 (s, CH_2); 0.33 (s, $SiMe_3$), as well as signals corresponding to starting material (10–15%). ^{13}C NMR ($CDCl_3$): 170.6 (C≡N);

155.3 (C3); 152.7 (C1); 129.7 (C5); 113.1 (C6); 106.0 (C4); C2 not obs.; 67.9 (OCH_2).

1,3-Bis[2-isocyano-3-(trimethylsiloxy)phenoxy]propane, SiNC-3. This reaction was carried out as for SiNC-2 using 0.574 g (1.85 mmol) of Dibenz-3, 38 ml THF, 1.70 ml (4.07 mmol) of 2.4 *M* n-BuLi, and 0.52 ml (0.45 g, 4.1 mmol) of $ClSiMe_3$. Upon workup of the dry reaction residue, a minimum amount of cold hexane was used to transfer the suspension of product and LiCl to a frit. The solid was washed with two 3-ml portions of cold hexane to remove impurities. The product was washed away from the LiCl with several portions of Et_2O into a clean Schlenk tube. The solvent was removed to give a yellow oil which crystallized upon addition of 1 ml of hexane. The mixture was cooled to −20°C, and the solution was decanted from the pale yellow solid. Washing of the solid with two 2-ml portions of cold hexane and drying in vacuo gave 0.45 g of the product (54%), m.p. 76–82°C. MS: M^+ (*m/e* 454, 0.4%); $(C_{10}H_{10}NO_2)^+$ (*m/e* 176, 14.2%); $[Si(CH_3)_3]^+$ (*m/e* 73, 100%). IR (Nujol mull): 2126 cm^{-1} s, ν(C≡N); 839 s, ν(SiO). ^1H NMR ($CDCl_3$): δ 7.17–6.45 (m, ArH); 4.29 (t, OCH_2); 2.36 (pentet, CH_2); 0.32 (s, $SiMe_3$). ^{13}C NMR ($CDCl_3$): 170.3 (C≡N); 155.3 (C3); 152.4 (C1); 129.6 (C5); 112.5 (C6); 109.7 (C2); 65.0 (OCH_2); 28.9 (CH_2).

Preparations of Rh complexes. [Rh(SiNC-3)$_2$]PF$_6$. A solution of $[Rh(COD)Cl]_2$ (0.091 g, 0.185 mmol) in 15 ml of benzene was treated dropwise with 0.501 g (1.10 mmol) of SiNC-3 in 20 ml of C_6H_6. The mixture was stirred overnight to give a yellow-green precipitate of $[Rh(SiNC\text{-}3)_2]Cl$ which was filtered, washed with C_6H_6, and dried in vacuo. This sample was dissolved in 8 ml of CH_2Cl_2 to give a deep green solution. To this was added a filtered solution of KPF_6 (0.080 g, 0.43 mmol) in 8 ml of CH_3CN. The mixture was stirred 15 min, and the solvent was removed at reduced pressure. The dark green residue was extracted with CH_2Cl_2. Removal of KCl by filtration, evaporation of the CH_2Cl_2 at reduced pressure and drying in vacuo gave the product as a green microcrystalline solid, 0.137 g (32%). IR (Nujol mull): 2159 cm^{-1} vs, ν(C≡N); 834 s, ν(PF) and ν(SiO). ^1H NMR (CD_2Cl_2): δ 7.30 (t, *J* 8.4 Hz, ArH); 6.61 (t, *J* 7.9 Hz, ArH); 4.30 (t, *J* 4.8 Hz, OCH_2); 2.47 (m, CH_2); 0.26 (s, $SiMe_3$). Anal. Found: C, 48.21; H, 5.03; N, 4.94. $C_{46}F_6H_{60}N_4O_8PRhSi_4$ calcd.: C, 47.74; H, 5.23, N, 4.84%.

[Rh$_2$(SiNC-2)$_4$](BPh$_4$)$_2$. A solution of SiNC-2 (0.159 g, 0.361 mmol) in 6 ml of C_6H_6 was added to a stirred solution of $[Rh(COD)Cl]_2$ (0.030 g, 0.061 mmol) in 8 ml of C_6H_6. The solution was stirred for 3.5 h. During this time a blue-green precipitate of $[Rh_2(SiNC\text{-}2)_4]Cl_2$ formed. The solid was filtered off, washed twice with 5 ml of C_6H_6 and dried in vacuo. Dichloromethane (9 ml) was added to the solid to give a deep blue-green solution. After being filtered, the solution was treated with a filtered solution of $NaBPh_4$ (0.050 g, 0.15 mmol) in 5 ml of CH_3CN. The resulting solution was stirred for 30 min, and solvents were removed at reduced pressure. The deep blue-green product, $[Rh_2(SiNC\text{-}2)_4](BPh_4)_2$, was extracted away from precipitated NaCl with CH_2Cl_2. After filtration, the solvent was slowly removed at reduced pressure, yielding the pure product as a deep blue-green glass (0.140 g, 88%). IR (Nujol mull): 2200 cm^{-1} w, sh; 2162 s, ν(C≡N); 840 s, ν(SiO). ^1H NMR (CD_2Cl_2): δ 7.35–6.09 (m, ArH); 4.27 (s, OCH_2); 0.13 (s, $SiMe_3$). Anal. Found: C, 62.49; H, 5.99; N, 4.29. $C_{136}H_{152}B_2N_8O_{16}Rh_2Si_8$ calcd.: C, 62.66; H, 5.88; N, 4.30%.

[Rh$_2$(SiNC-2)$_4$](PF$_6$)$_2$. A sample of $[Rh_2(SiNC\text{-}2)_4]Cl_2$ was prepared from 0.565 g (1.28 mmol) of SiNC-2 (10 ml of C_6H_6) and 0.104 g (0.211 mmol) of $[Rh(COD)Cl]_2$ (15 ml of C_6H_6) as outlined for $[Rh_2(SiNC\text{-}2)_4](BPh_4)_2$. A similar

metathesis procedure employing 0.086 g (0.47 mmol) of KPF_6 gave $[Rh_2(SiNC\text{-}2)_4](PF_6)_2$ as a deep blue-green solid, 0.335 g (70%). IR (Nujol mull): 2200 cm^{-1} w, sh, 2160 vs, ν(C≡N); 842 vs, ν(PF) and ν(SiO). ^1H NMR (CD_3CN): δ 7.05–6.37 (m, ArH); 4.35 (s, OCH_2); 0.16 (s, $SiMe_3$). Anal. Found: C, 46.80; H, 5.02; N, 4.97. $C_{88}H_{112}F_{12}N_8O_{16}P_2Rh_2Si_8$ calcd.: C, 46.80; H, 5.00; N, 4.96%.

Acknowledgement

This research was supported by the National Science Foundation (Grant No. CHE78-07913 to R.J.A.) and the U.S. Department of Energy, Office of Basic Energy Sciences, Materials Sciences Division (to R.A.J.). We thank James W. Richardson, Jr. for assistance with the X-ray results.

References

1 R.J. Angelici, M.H. Quick and G.A. Kraus, Inorg. Chim. Acta, 44 (1980) L137.
2 R.A. Michelin and R.J. Angelici, Inorg. Chem., 19 (1980) 3853.
3 R.J. Angelici, M.H. Quick, G.A. Kraus and D.T. Plummer, Inorg. Chem., 21 (1982) 2178.
4 M.L. Winzenburg, J.A. Kargol and R.J. Angelici, J. Organomet. Chem., 249 (1983) 415.
5 J.A. Kargol and R.J. Angelici, Inorg. Chim. Acta, 68 (1983) 127.
6 R.A. Michelin and R.J. Angelici, Inorg. Chem., 19 (1980) 3850.
7 N.S. Lewis, K.R. Mann, J.G. Gordon II and H.B. Gray, J. Am. Chem. Soc., 98 (1976) 7461.
8 K.R. Mann, J.G. Gordon II and H.B. Gray, J. Am. Chem. Soc., 97 (1975) 3553.
9 K. Kawakami, M. Okajima and T. Tanaka, Bull. Chem. Soc. Jpn., 51 (1978) 2327.
10 K.R. Mann, N.S. Lewis, R.M. Williams, H.B. Gray and J.G. Gordon II, Inorg. Chem., 17 (1978) 828.
11 P.V. Yaneff and J. Powell, J. Organomet. Chem., 179 (1979) 101.
12 H. Endres, N. Gottstein, H.J. Keller, R. Martin, W. Rodemeyer and W. Steiger, Z. Naturforsch. B, 34 (1979) 827.
13 K.R. Mann, J.A. Thich, R.A. Bell, C.L. Coyle and H.B. Gray, Inorg. Chem., 19 (1980) 2462.
14 J.M. Robertson and J.G. White, J. Chem. Soc., (1945) 607.
15 F.H. Herbstein in J.D. Dunitz and J.A. Ibers (Eds.), Perspectives in Structural Chemistry, Vol. IV, J. Wiley and Sons, New York 1971, p. 166.
16 J.A. Ibers, L.J. Pace, J. Martinsen and B.M. Hoffman, Struct. and Bonding, 50 (1982) 1.
17 R. Schröder, U. Schöllkopf, E. Blüme and I. Hoppe, Liebigs Ann. Chem., (1975) 533.
18 I. Ugi and R. Meyr, Chem. Ber., 93 (1960) 239.
19 A.L. Balch and J. Miller, J. Organomet. Chem., 32 (1971) 263.
20 R.V. Parish and P.G. Simms, J. Chem. Soc. Dalton Trans., (1972) 809.
21 J.W. Dart, M.K. Lloyd, R. Mason and J.A. McCleverty, J. Chem. Soc. Dalton Trans., (1973) 2039.
22 G.L. Geoffroy, H. Isci, J. Litrenti and W.R. Mason, Inorg. Chem., 16 (1977) 1950.
23 Y. Ohtani, S. Miya, Y. Yamamoto and H. Yamazaki, Inorg. Chim. Acta, 53 (1981) L53.
24 Y. Yamamoto, K. Aoki and H. Yamazaki, Inorg. Chem., 18 (1979) 1681.
25 R.A. Jacobson, J. Appl. Crystallogr., 9 (1976) 115.
26 W.J. Rohrbaugh and R.A. Jacobson, Inorg. Chem., 13 (1974) 2535.
27 R.L. Lapp, Ph.D. Dissertation, Iowa State University, Ames, Iowa, USA, 1979.
28 S.L. Lawton and R.A. Jacobson, Inorg. Chem., 7 (1968) 2124.
29 R.L. Lapp and R.A. Jacobson, Ames, Iowa, Aug. 1979, DOE Report 1S-4708.
30 D.R. Powell and R.A. Jacobson, Ames, Iowa, April, 1980, DOE Report 1S-2155.
31 D.W.J. Cruickshank and D.E. Pilling in R. Pepinsky, J.M. Roberts and J.C. Speakman (Eds.), Computing Methods and the Phase Problem in X-ray Crystal Analysis, Pergamon Press, New York, New York, 1961, p. 45–46.
32 H.P. Hanson, F. Herman, J.D. Lea and S. Skillman, Acta Crystallogr., 17 (1960) 1040.
33 D.H. Templeton in C.H. McGillavry, G.D. Riek and K. Lonsdale (Eds.), International Tables for X-ray Crystallography, Vol. III, Kynoch Press, Birmingham, England, 1962, Table 3.3.2.C.
34 R.F. Stewart, E.R. Davidson and W.T. Simpson, J. Chem. Phys., 42 (1965) 3175.
35 J. Chatt and L.M. Venanzi, J. Chem. Soc. A, (1957) 4735.
36 E. Sorkin, W. Roth and H. Erlenmeyer, Helv. Chim. Acta, 35 (1952) 1736.
37 D.F. Shriver, The Manipulation of Air-Sensitive Compounds, McGraw-Hill, New York, 1969, p. 141–158.